Optically Active Photochromic Polymers with Three-Arm Star Structure by Atom Transfer Radical Polymerization

Luigi Angiolini,* Tiziana Benelli, Loris Giorgini, and Elisabetta Salatelli

Dipartimento di Chimica Industriale e dei Materiali and INSTM UdR−Bologna, University of Bologna, Viale Risorgimento 4, 40136 Bologna, Italy

Received January 21, 2006; Revised Manuscript Received March 29, 2006

ABSTRACT: Atom transfer radical polymerization has been applied for the first time to synthesize optically active, photochromic methacrylic polymers having three-arm star structure, starting from a central core of C_3 symmetry that can be used to investigate the conformational origin of chirality in this class of synthetic materials. By just changing the duration of the polymerization process, star-shaped macromolecules with distinct average chain lengths, low polydispersity values, and well-defined end groups have been obtained. The so-obtained polymers, fully characterized by spectroscopic and thermal techniques, exhibit relevant specific optical rotations and chiroptical properties with respect to the reference monomeric model compound as well as to the related linear derivatives previously investigated. This behavior is attributed to the stiffness of aromatic core, which limits the free movement of one chain end, thus favoring the macromolecules to assume a more elevated conformational rigidity with respect to the linear samples of comparable average chain length.

Introduction

An intense interest is currently arisen to investigations dealing with the amplification of chirality of polymeric materials, in solution as well as in the solid state.[1−3]

In previous studies we have reported the synthesis and the characterization of optically active photochromic methacrylic polymers bearing in the side chain both a chiral group of one single configuration and the trans-azoaromatic moiety with a strongly conjugated electron donor−acceptor system.[4−9] This functional combination allows the polymers to display both the properties typical of dissymmetric systems (optical activity, absorption of circularly polarized light in the UV−vis spectral region)[10] as well as the features of photochromic materials (NLO properties, photoresponsiveness, photorefractivity).[11,12] Thus, these materials can be considered of potential interest for technological applications, such as optical storage, waveguides, chemical photoreceptors, etc.[13−15]

On the other hand, the induction of helical handedness in polymers or oligomers has attracted widespread interest because of its possible applications in optical devices or data storage and also because of its relevance to chiral amplification as it may have occurred at the early stages of life on earth. We have observed that it is also possible to reversibly photomodulate the chiroptical properties of thin films of these chiral photochromic polymers bearing side-chain permanent dipole azobenzene chromophores by irradiation with circularly polarized (CP) light of one single L or R rotation sense.[16,17]

We recently synthesized by atom transfer radical polymerization (ATRP)[18,19] a series of linear optically active methacrylic homopolymers poly[(*S*)-3-methacryloyloxy-1-(4-azobenzene)-pyrrolidine] [poly[(*S*)-MAP] (Figure 1), with different average polymerization degree and low polydispersity, bearing in the side chain the pyrrolidinyl group of one single configuration linked through the nitrogen atom to the azobenzene chromophore. The results indicated that the chirality of these macromolecules is due to conformational effects and strongly depends on their average chain length, the corresponding monomeric model (*S*)-PAP (Figure 1) displaying very low optical activity.[8]

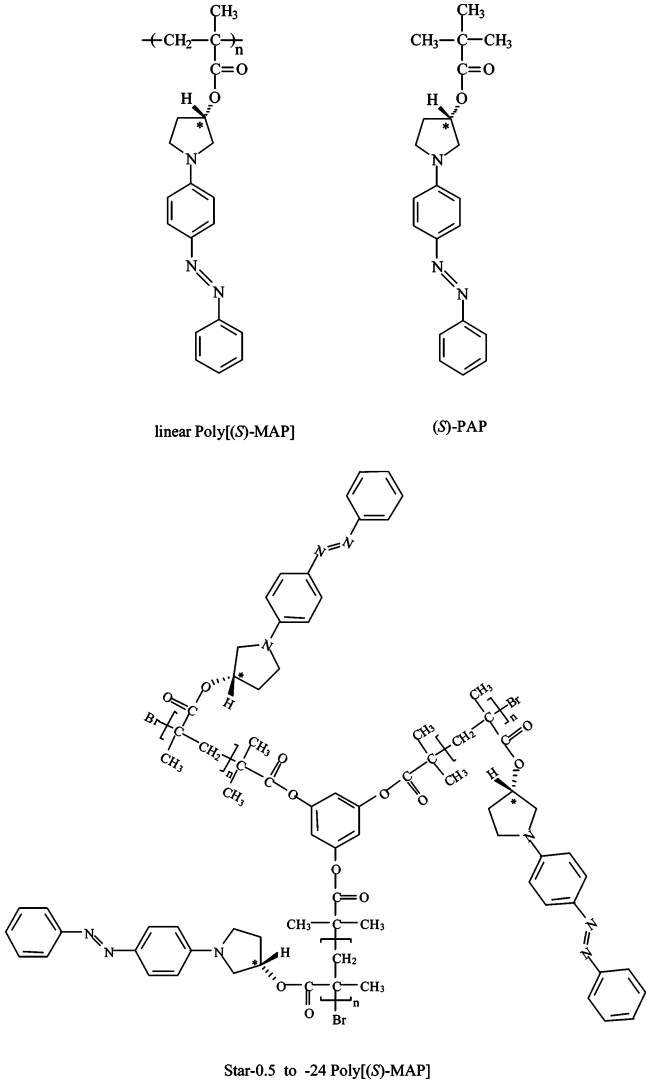

Figure 1. Chemical structures of model compound (*S*)-PAP and linear and star poly[(*S*)-MAP] polymers.

* Corresponding author: Tel and Fax +39 051 2093687; e-mail luigi.angiolini@unibo.it.

10.1021/ma060148o CCC: $33.50
Published on Web 05/06/2006

This finding has been confirmed by studies on the dimeric derivative 2,4-dimethylglutaric acid bis(*S*)-3-[1-(4′-nitro-4-azobenzene)pyrrolidine ester,[20] corresponding to the smallest section of the polymeric chain where interchromophore interactions are relevant. Its CD spectrum shows an exciton couplet of strong amplitude (about a third of the signal measured for the related polymer[8] having $\bar{M}_n = 31\,500$), which suggests that the chiral interactions between a couple of chromophores in solution are already important and that the optical activity of these materials should be substantially related to relatively short chain sections with conformational dissymmetry of one prevailing screw sense.

With the aim to investigate further into the structure−property relationships in these materials, we have considered of interest to synthesize and characterize the corresponding polymers with a star structure consisting of three linear chains linked to a central aromatic core of C_3 symmetry (star-0.5 through star-24, where the figure refers to hours of polymerization duration) (Figure 1).

Investigations on star polymers have become of interest in recent years because of their unique properties and important applications.[21,22] However, to our knowledge only one optically active C_3 star polymer is reported by Wulff and Zweering[23] as obtained by coupling of three isotactic poly(methyl methacrylate) reactive chains (cryptochiral at a polymerization degree >300) with 1,3,5-benzenetricarbonyl chloride.

Chiral dendrimers,[24−26] supramolecular helical polymers,[3] and optically active low molecular weight compounds with C_3 symmetry have found increasing interest in recent times because they are expected to become useful in chemical operations including asymmetric catalysis, chiral recognition, and resolution.[27,28] This field has been accurately reviewed by Moberg.[29]

An efficient method for the synthesis of star polymers is living polymerization, which provides a satisfactory control of both molecular structure and molecular weight. In the past, the most used approach was anionic polymerization, but in recent years the living radical techniques have gained interest because they are tolerant toward impurities present in solvent and reactants, including water, and can be employed with a wide range of vinyl monomers.[30−33]

Accordingly, we have polymerized the monomer (*S*)-(+)-3-methacryloyloxy-1-(4-azobenzene)pyrrolidine [(*S*)-MAP] by ATRP, using 1,3,5-(2′-bromo-2′-methylpropionato)benzene (BMPB) as the initiator of radical living polymerization and the transition metal salt Cu(I)Br, in combination with 1,1,4,7,-10,10-hexamethyltriethylenetetramine (HMTETA) as ligand. This method has allowed us to obtain macromolecules having the same C_3-symmetrical aromatic central core and various average chain lengths with sufficiently low polydispersity values just by varying the process duration.

Optical activity, electronic spectra, and thermal properties of the obtained products have been compared with those displayed by the corresponding linear poly[(*S*)-MAP]s, previously obtained by various methods,[8,18,19] in order to achieve indications about the effects originated in the system by the star-shaped molecular architecture.

Experimental Section

Physicochemical Measurements. ^{1}H and ^{13}C NMR spectra were obtained at room temperature, on 5−10% $CDCl_3$ solutions, using a Varian NMR Gemini 300 spectrometer. Chemical shifts are given in ppm from tetramethylsilane (TMS) as the internal reference. ^{1}H NMR spectra were run at 300 MHz by using the following experimental conditions: 24 000 data points, 4.5 kHz spectral width, 2.6 s acquisition time, 128 transients. ^{13}C NMR spectra were recorded at 75.5 MHz, under full proton decoupling, by using the following experimental conditions: 24 000 data points, 20 kHz spectral width, 0.6 s acquisition time, 64 000 transients.

FT-IR spectra were carried out on a Perkin-Elmer 1750 spectrophotometer, equipped with an Epson Endeavour II data station, on sample prepared as KBr pellets.

UV−vis absorption spectra were recorded at 25 °C in the 700−250 nm spectral region with a Perkin-Elmer Lambda 19 spectrophotometer on $CHCl_3$ solutions by using cell path lengths of 0.1 cm. Concentrations in azobenzene chromophore of about 3×10^{-4} mol L^{-1} were used.

Optical activity measurements were accomplished at 25 °C on $CHCl_3$ solutions ($c \approx 0.250$ g dL^{-1}) with a Perkin-Elmer 341 digital polarimeter, equipped with a Toshiba sodium bulb, using a cell path length of 1 dm. Specific $\{[\alpha]_D^{25}\}$ and molar $\{[\Phi]_D^{25}\}$rotation values at the sodium D line are expressed as deg dm^{-1} g^{-1} cm^3 and deg dm^{-1} mol^{-1} dL, respectively.

Circular dichroism (CD) spectra were carried out at 25 °C on $CHCl_3$ solutions on a Jasco 810 A dichrograph, using the same path lengths and solution concentrations as for the UV−vis measurements. $\Delta\epsilon$ values, expressed as L mol^{-1} cm^{-1}, were calculated from the following expression: $\Delta\epsilon = [\Theta]/3300$, where the molar ellipticity $[\Theta]$ in deg cm^2 $dmol^{-1}$ refers to one azobenzene chromophore.

Number-average molecular weights of the polymers ($\bar{M}_n$) and their polydispersity indexes ($\bar{M}_w/\bar{M}_n$) were determined in THF solution by SEC using HPLC Lab Flow 2000 apparatus, equipped with an injector Rheodyne 7725i, a Phenomenex Phenogel 5 μm MXL column, and a UV−vis detector Linear Instrument model UVIS-200, working at 254 nm. A calibration curve for the MXL column was obtained by using monodisperse polystyrene standards in the range 800−35 000.

The glass transition temperature values were determined by differential scanning calorimetry (DSC) on a TA Instruments DSC 2920 modulated apparatus at a heating rate of 10 K/min under nitrogen atmosphere on samples weighing 5−9 mg. Checking of the liquid crystalline behavior was carried out with a Zeiss Axioscope2 polarizing microscope through crossed polarizers fitted with a Linkam THMS 600 hot stage.

The initial thermal decomposition temperature (T_d) was determined with a Perkin-Elmer TGA-7 thermogravimetric analyzer by heating the samples in air at a rate of 20 °C/min.

Materials. The monomer (*S*)-(+)-3-methacryloyloxy-1-(4-azobenzene)pyrrolidine [(*S*)-MAP] and the model compound (*S*)-(+)-3-pivaloyloxy-1-(4-azobenzene)pyrrolidine [(*S*)-PAP] were synthesized as previously reported.[8] Chloroform and THF were purified and dried according to the reported procedures[34] and stored under nitrogen. The trifunctional initiator 1,3,5-(2′-bromo-2′-methylpropionato)benzene (BMPB) was prepared as previously described;[35,36] 1,1,4,7,10,10-hexamethyltriethylenetetramine (HMTETA), copper bromide, and all the other reagents and solvents (Aldrich) were used as received.

Synthesis of C_3-Symmetrical Polymers by ATRP. All homopolymerizations of (*S*)-MAP were carried out in glass vials using BMPB as the initiator, HMTETA as the ligand, and Cu(I)Br as catalyst in dry THF [(*S*)-MAP/THF 1/20 g/mL]. Each mixture [(*S*)-MAP/BMPB/HMTETA/CuBr = 150:1:3:3 by mol] was introduced into several vials under a nitrogen atmosphere, submitted to several freeze−thaw cycles and heated at 60 °C. To terminate the polymerization reaction, the vials were frozen in liquid nitrogen after known reaction times, ranging from 30 min to 24 h, and the obtained product was purified by precipitation in a large excess of methanol. The solid polymers (Star-0.5 through Star-24) were finally dried at 70 °C under vacuum for several days to constant weight. Relevant data for the synthesized derivatives are reported in Table 1. All the products were characterized by FT-IR, ^{1}H NMR, and ^{13}C NMR. As an example, the spectroscopic data for Star-1, obtained after 1 h of reaction, are here reported.

^{1}H NMR ($CDCl_3$): 8 00−7.65 (m, 4H, arom 2′-H and meta to amino group), 7.35 (m, 3H, arom 3′-H and 4′-H), 6.60 (3H, CH

Table 1. Characterization Data of Star Polymeric Derivatives

samples	reaction time (h)	yield[a] (%)	$\bar{M}_{n,SEC}$[b] (g/mol)	$\bar{M}_w/\bar{M}_n$[b]	$[\alpha]_D^{25}$	$[\Phi]_D^{25}$ [c]	T_g[d] (°C)	T_d[e] (°C)
star-0.5	0.5	10.0	4 500	1.28	+217	+728	115	237
star-1	1	17.5	7 800	1.22	+306	+1026	136	260
star-2	2	30.0	10 500	1.16	+341	+1144	140	266
star-4	4	40.0	15 200	1.15	+396	+1328	161	289
star-8	8	51.2	16 600	1.16	+403	+1352	163	290
star-24	24	63.9	18 900	1.19	+429	+1476	156	293
linear-24[f]	24	67.7	10 000	1.4	+428	+1434	160	295
poly[(*S*)-MAP][g]	72	69	31 500	1.6	+410	+1374	169	314

[a] Calculated as (g of polymer/g of monomer) × 100. [b] Determined by SEC in THF at 25 °C. [c] Molar optical rotation, calculated as ($[\alpha]_D^{25} \times M/100$), where M represents the molecular weight of one repeating unit of poly[(*S*)-MAP]. [d] Determined by DSC. [e] Determined by TGA. [f] Reference 18: obtained by ATRP. [g] Reference 8: obtained by AIBN initiated polymerization.

arom core), 6.50 (m, 2H, arom ortho to amino group), 5.40−4.55 (m, 1H, 3-CH), 3.70−3.00 (m, 4H, 2- and 5-CH_2), 2.30 (2H, CH_2−C−Br), 2.40−1.40 (m, 4H, 4-CH_2 and main chain CH_2), 1.95 (3H, CH_3−C−Br), 1.40−0.50 ppm (m, 3H, main chain CH_3 and 18H, $C(CH_3)_2$−COO).

^{13}C NMR ($CDCl_3$): 177.1 (CO repeating unit), 168.5 (CO core), 153.6, 149.8, 144.5 (arom *C*−N═N−*C* and *C*−N−CH_2), 152.4 (arom *C*−O core), 130.2 (arom 4′-C), 129.6 (arom 3′-C), 125.8, 122.9 (arom 2′-C and 3-C), 113.1 (arom *C*−H core), 112.3 (arom 2-C), 75.6 (*C*H−O), 59.3 (*C*(CH_3)−Br), 55.0 (main chain CH_2−*C*), 53.1 (CH−CH_2−N), 46.3 (CH_2−CH_2−N), 45.5 (main chain *C*H_2−C), 42.5 (*C*(CH_3)$_2$−CH_2), 38.2 (*C*H_2−C(CH_3)−Br), 31.1 (CH-*C*H_2−CH_2), 28.1 (C(*C*H_3)−Br), 23.4 (C(*C*H_3)$_2$−CH_2), 19.9 and 17.4 ppm (main chain CH_3).

FT-IR (KBr): 3063 (ν_{CH}, arom), 2978, 2852 (ν_{CH}, aliph), 1728 (ν_{CO}, ester of the repeating unit and arom core), 1602 and 1514 ($\nu_{C=C}$, arom), 1139 (ν_{C-O}), 819 (δ_{CH}, 1,4-disubst arom ring), 765, 689 cm^{-1} (δ_{CH}, monosubst arom ring).

Results and Discussion

Synthesis and Characterization. The ATRP process occurs in the presence of halide as initiator and a metal atom with complexing ligands in a low oxidation state. The propagation of the process involves successive alternating transfer of the halide from the dormant polymer chain to the ligated metal complex to give a dynamic equilibrium between active and dormant species. Starting from a trifunctional initiator (BMPB), this technique allows to obtain macromolecules with well-defined star structure, in terms of arms number and chain length.

The occurrence of polymerization involving the methacrylic double bond was confirmed by FT-IR, showing the disappearance of the band at 1634 cm^{-1}, related to the stretching vibration of the double bond in the monomer, and the shift of the estereal carbonyl stretching frequency from 1709 cm^{-1} in the monomer, to higher frequencies (1728 cm^{-1}) in the polymer, due to the reduced electron delocalization determined by the reaction of the methacrylic double bond.

Accordingly, in the ^{1}H NMR spectra of all samples, the resonances at 5.60 and 6.10 ppm related to the vinylidenic protons of monomer (*S*)-MAP are absent, and the methyl resonances are shifted from about 1.95 ppm to higher field.

In addition, the samples obtained at lower reaction times (Star-0.5 and Star-1) display the resonances of the methylic protons of the BMPB residue at 1.3 ppm and the signals related to methylene and methyl groups bonded to the quaternary carbon atom bearing the terminal Br atom at 1.9 and 2.3 ppm, respectively. Their intensity decreases by increasing the reaction time and becomes progressively obscured by the more intense resonances related to the aliphatic protons of the main chain, thus preventing to assess the number-average molecular weight of each sample directly by integration of the NMR signals.

Analogous considerations are valid for the singlet signal of the aromatic core at 6.60 ppm, overlapped to the signals of the azo-aromatic protons in ortho position to pyrrolidinic amino group.

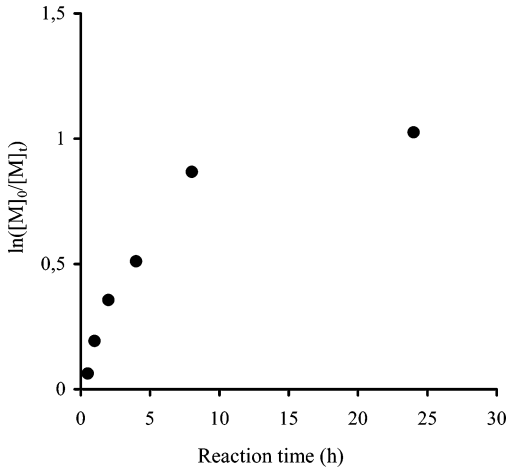

Figure 2. Time dependence of $\ln([M]_0/[M]_t)$ in the ATRP of (*S*)-MAP in THF.

The living character of the polymerization is confirmed by ^{13}C NMR spectra, which display signals related to the quaternary carbon atom bonded to Br at 59.3 ppm and to the methyl and methylene carbon atoms of the growing chain end group at 28.1 and 38.2 ppm, respectively.

Figure 2 shows the relationship between $\ln([M]_0/[M]_t)$ (where $[M]_0$ and $[M]_t$ are the initial and at t time monomer concentration, respectively) and the reaction time, indicating that the reaction rate follows a first-order kinetics throughout the first 4 h of the process and then decreases for conversions over 50%. A similar behavior has been previously reported[33] for the ATRP of methyl acrylate starting from a multifunctional initiator and attributed to the irreversible conversion of the catalyst from Cu(I) to Cu(II) during the process, which results in an increase of the polydispersity index.

In our case, however, the values of $\bar{M}_w/\bar{M}_n$ measured by SEC are almost constant (in the range 1.1−1.3), as reported in Table 1; thus, the decrease of the polymerization rate at longer reaction times could be attributed to increase of viscosity and decrease of monomer concentration in the reaction solution. Moreover, as yields and number-average molecular weight values of the obtained polymers show a strong dependence on the reaction time (Table 1), by varying this last parameter only, it is actually possible to modulate the macromolecular chain length, as shown by SEC chromatograms reported in Figure 3.

The plot of the number molecular average weight of the resulting star-shaped polymers as determined by SEC ($\bar{M}_{n,SEC}$) against monomer conversion is shown in Figure 4. The theoretical values of $\bar{M}_n$ ($\bar{M}_{n,th}$), which are valid only in the

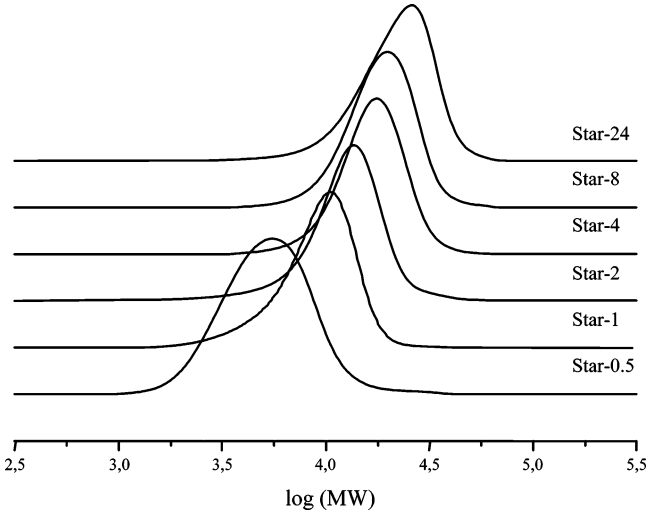

Figure 3. Normalized molecular weight distributions of star polymers as determined by SEC in THF at 25 °C.

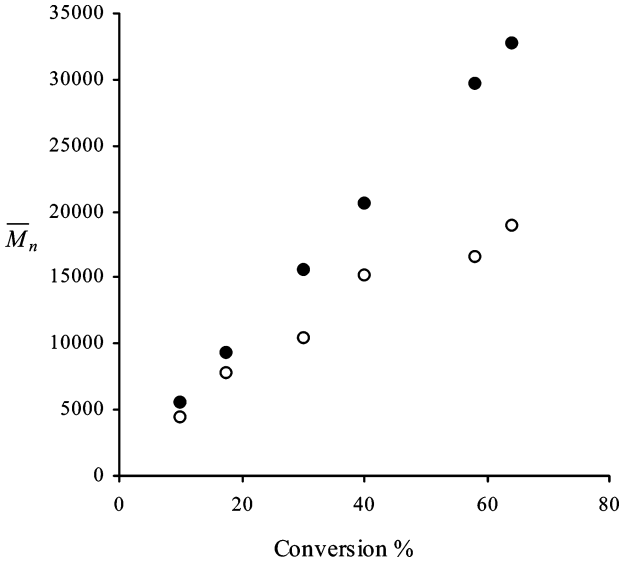

Figure 4. Evolution of the number-average molecular weight determined by SEC in THF at 25 °C (○) and calculated values (●) vs monomer conversion in the ATRP of (*S*)-MAP.

absence of chain termination and transfer reactions, may be calculated by the following equation:[32]

$$\bar{M}_{n,th} = \text{conversion} \times (M_{(S)\text{-MAP}}/M_{BMPB})MW_{(S)\text{-MAP}} + MW_{BMPB} \quad (1)$$

where $M_{(S)\text{-MAP}}$ and M_{BMPB} are the initial amounts in moles of monomer and trifunctional initiator and $MW_{(S)\text{-MAP}}$ and MW_{BMPB} are their molecular weights, respectively. As reported in Figure 4, calculated and SEC values are coincident only at low values of conversion, but increasing the conversion, they appear progressively divergent. Having performed the ATRP of (*S*)-MAP with one-third molar amount of initiator with respect to the corresponding synthesis of the related linear derivative[18] linear-24 (Table 1), a $\bar{M}_{n,th}$ of 32 700 g/mol from eq 1 and $\bar{M}_{n,SEC}$ around 28 000 g/mol were expected for star-24, if termination and chain transfer occurred to the same extent. The experimental value of $\bar{M}_{n,SEC}$ 18 900 g/mol found for star-24 (Table 1) indicates therefore that, in addition to termination reactions taking place under the real polymerization conditions, the increasing of rigidity of the helical conformations and the particular molecular structure of star-shaped polymers are responsible of this finding. It is well-known, in fact, that, due to their smaller hydrodynamic volume with respect to that of linear polystyrenes having the same molecular weight, SEC analysis gives underestimated molecular weight values of star-shaped polymers when measured with reference to the usually adopted linear polystyrene standards.[37,38]

The approximately linear correlation between $\bar{M}_{n,SEC}$ and monomer conversion is indicative of the living character of the ATRP process, and SEC analysis proves to be useful to confirm that a steady increment of the average molecular weight with conversion has taken place. In conclusion, all the instrumental characterization techniques confirm that three-arms star polymers with C_3 symmetry and varying molecular size have been successfully obtained.

Thermal Properties. The thermal characterizations of all polymeric samples were performed by thermogravimetric analysis (TGA) and by differential scanning calorimetry (DSC) (Table 1). The polymers exhibit good thermal stability, with initial weight losses values in air (T_d) that increase with the average molecular weight to level off at the value of 290 °C for $\bar{M}_n$ around 15 000 g/mol.

This behavior differs from that shown by their linear counterparts[18,19] having T_d values substantially constant (around 300 °C) with the average molecular weight, indicating the presence of a branching effect in the star-shaped derivatives. Similarly, a decrease of T_d, T_g, and melting point with the increase of the number of arms was reported for star-shaped polylactide.[39]

Only second-order transitions originated by glass transitions with no melting peaks are observed in the DSC thermograms, thus suggesting that these macromolecules are substantially amorphous in the solid state, the absence of liquid crystalline behavior being also noted upon observation with a polarizing microscope. The T_g values of star-0.5 to star-8 increase from about 115 to 163 °C (Table 1), thus showing a very similar behavior to linear poly[(*S*)-MAP][18,19] and approaching the maximum value of 169 °C found for poly[(*S*)-MAP][8] with $\bar{M}_n$ = 31 500, obtained by AIBN-initiated free radical polymerization. As expected, the increase of the average molecular weight appears to strongly reduce the mobility of polymeric chains as a consequence of the increased extent of interchromophore interactions. However, the sample star-24 displays a somewhat reduced value of T_g, possibly in consequence of increased polydispersity index with of lower degree of molecular size distribution.

Both the good thermal stability and high values of T_g suggest that these polymeric systems, although possessing a low average molecular weight, may be promising for solid-state applications in optoelectronics due to their stability at room temperature subsequently to photo- or electrically induced orientation of the azoaromatic dipoles.

UV−Vis Properties. The star polymers in $CHCl_3$ solution display UV−vis spectra (Table 2) similar to those of the analogous linear compounds previously synthesized by ATRP from the monofunctional initiator ABIB.[15] This behavior suggests that the electronic absorption properties in dilute solution of this class of polymers are unaffected by branching. In the 250−700 nm spectral region (Figure 5a), in fact, they exhibit two absorption bands, centered around 409 and 259 nm: the former one, more intense, attributed to electronic transitions such as $n-\pi^*$, $\pi-\pi^*$ and internal charge transfer of the azobenzene chromophore, and the latter to the $\pi-\pi^*$ electronic transition of the aromatic ring.[40]

Table 2. UV−Vis Spectra of (*S*)-PAP and Linear and Star Poly[(*S*)-MAP] Polymers in $CHCl_3$ Solution at 25 °C

	first absorption band		second absorption band	
samples	λ_{max} [a]	$\epsilon_{max} \times 10^{-3}$ [b]	λ_{max} [a]	$\epsilon_{max} \times 10^{-3}$ [b]
(*S*)-PAP[c]	409	29.8	258	11.6
poly[(*S*)-MAP][c]	409	26.9	259	11.0
star-0.5	409	26.9	259	11.0
star-1	408	27.0	260	10.8
star-2	408	26.9	258	10.6
star-4	409	26.9	259	10.8
star-8	408	27.0	259	10.9
star-24	408	27.1	260	10.9

[a] Wavelength of maximum absorbance, expressed in nm. [b] Expressed in L mol^{-1} cm^{-1} and calculated for one single chromophore. [c] Reference 8.

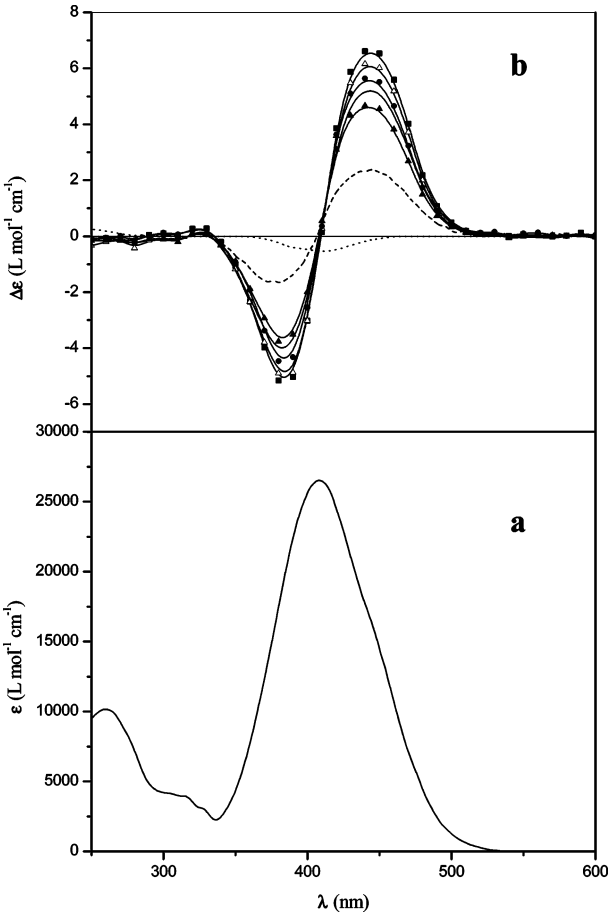

Figure 5. UV−vis spectrum of star-2 (a) and CD spectra (b) of (*S*)-PAP (···), star-0.5 (- - -), star-1 (▲), star-2 (−), star-4 (●), star-8 (△), and star-24 (■) polymers in $CHCl_3$ solution.

A significant hypochromism was formerly observed for both the first and the second band when passing from the model (*S*)-PAP to the corresponding polymer poly[(*S*)-MAP],[8] regardless the solvent employed. Similar behavior was previously reported for several polymers[41−43] and the dimeric derivative[20] and attributed to the occurrence of electrostatic dipole−dipole interactions between the neighboring aromatic chromophores.[20,44−46]

As shown in Table 2, the molar absorption coefficient values related to the first absorption band of star-0.5 through star-24 are all lower, around 27.0×10^{-3} L mol^{-1} cm^{-1}, than in the model compound (*S*)-PAP, with no apparent dependence on the average polymerization degree of the sample. Very similar values (in the range $25.4-26.8 \times 10^{-3}$ L mol^{-1} cm^{-1}) have

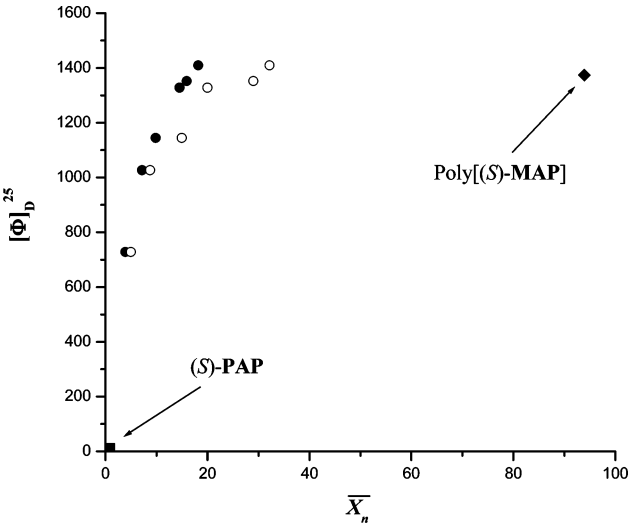

Figure 6. Evolution of the molar optical rotation vs $\bar{X}_{n,SEC}$ (●) and $\bar{X}_{n,th}$ (○) of the star polymers. The related values of (*S*)-PAP (■) and linear poly[(*S*)-MAP] with $\bar{M}_n = 31\,500$ (◆) are also represented.[8]

also been recently observed for the analogous linear derivatives obtained by ATRP,[18] thus suggesting that the hypochromism shown in dilute solution by methacrylic polymers bearing in the side-chain azobenzene groups is mainly due to the presence of intrachain interactions taking place between adjacent chromophores whereas the interchain ones are irrelevant.

Optical Activity, CD Spectra, and Chiroptical Properties. With the aim to assess the dependence of the optical activity on the average molecular weight of the materials prepared, the specific $\{[\alpha]_D^{25}\}$ and molar $\{[\Phi]_D^{25}\}$ optical rotation of all samples with different average polymerization degree $\bar{X}_n$ (referred to each macromolecular chain linked to the central core) have been determined in $CHCl_3$ solution (Table 1 and Figure 6).

As shown in Figure 6, all polymeric products display increasing optical activity with the average polymerization degree measured by SEC ($\bar{X}_{n,SEC}$) and the theoretical value ($\bar{X}_{n,th}$) as calculated by eqs 2 and 3, respectively:

$$\bar{X}_{n,SEC} = (\bar{M}_{n,SEC} - MW_{BMPB})/3MW_{(S)\text{-MAP}} \quad (2)$$

$$\bar{X}_{n,th} = (\bar{M}_{n,th} - MW_{BMPB})/3MW_{(S)\text{-MAP}} \quad (3)$$

This behavior, previously observed for the analogous linear derivatives prepared by both free radical polymerization[8] and ATRP,[18,19] suggests that even a few adjacent chiral units are also able to produce a remarkable increase of optical activity in these differently structured macromolecules.

The enhanced optical activity of star-shaped derivatives with respect to the linear polymers could in principle be ascribed also to the occurrence of main-chain stereoregularity originated by a prevalent microtacticity of the repeating units. An evaluation of the microtacticity of all the polymeric derivatives has been made based on the ^{13}C NMR signals of the methacrylic methyl group, which displays two resonances located at ≈19.8 and 17.4 ppm, assigned to *mr* (meso-racemo) and *rr* (racemo-racemo) heterotactic and syndiotactic triads, respectively.[47] Assuming that the polymerization process follows a Bernoullian statistics, the probabilities of formation of a meso dyad *m* (P_m) can be calculated from the integrated signals ratio (*mr*/*rr*), which corresponds to $2P_m(1 - P_m)/(1 - P_m)^2$, i.e., to the ratio between the probability of formation of *mr* and *rr* triads.[48] The results for the series of star polymers ($P_m = 0.25-0.29$), as reported

Table 3. Microtacticity of Polymeric Derivatives As Determined by ^{13}C NMR[a]

sample	P_m	P_r	*mm* (%)	*mr*(*rm*) (%)	*rr* (%)	$P_{m/r}$	$P_{r/m}$	$P_{m/m}$	$P_{r/r}$
poly[(*S*)-MAP][b]	0.26	0.74	7	38	55	0.26	0.73	0.27	0.74
star-0.5	0.29	0.71	8	41	51	0.29	0.71	0.26	0.73
star-1	0.28	0.72	8	40	52	0.28	0.73	0.29	0.72
star-2	0.25	0.75	7	38	56	0.25	0.75	0.25	0.75
star-4	0.28	0.72	8	40	52	0.28	0.73	0.28	0.72
star-8	0.26	0.74	7	39	55	0.26	0.74	0.26	0.74
star-24	0.27	0.73	7	40	53	0.27	0.73	0.27	0.73
linear-2[c]	0.27	0.73	7	39	54	0.27	0.73	0.27	0.73
linear-8[c]	0.29	0.71	9	41	50	0.29	0.71	0.29	0.71
linear-24[c]	0.26	0.74	7	39	55	0.26	0.74	0.26	0.74

[a] P_m and P_r represent the probability of formation of *meso* and *racemo* dyads, respectively; *mm*, *mr*(*rm*) and *rr* are the percent amounts of triads present in the polymers; $P_{m/r}$, $P_{r/m}$, $P_{m/m}$, and $P_{r/r}$ are the calculated probabilities that a given dyad follows a dyad having the same or the opposite relative configuration. [b] Reference 8: obtained by AIBN initiated polymerization. [c] Reference 18: obtained by ATRP after 2, 8, and 24 h reaction.

Table 4. CD Spectra of (*S*)-PAP and Linear and Star Poly[(*S*)-MAP] Polymers in $CHCl_3$ Solution at 25 °C

	first absorption band					second absorption band	
samples	λ_1[a]	$\Delta\epsilon_1$[b]	λ_0[c]	λ_2[a]	$\Delta\epsilon_2$[b]	λ_3[a]	$\Delta\epsilon_3$[b]
(*S*)-PAP[d]	410	−0.51				258	+0.22
poly[(*S*)-MAP][d]	445	+ 7.35	409	384	−2.30	258	−0.32
star-0.5	444	+3.31	407	384	−3.79	258	−0.15
star-1	443	+4.73	408	383	−4.15	258	−0.20
star-2	443	+5.25	408	384	−4.57	258	−0.19
star-4	444	+5.62	409	385	−5.11	258	−0.25
star-8	444	+6.15	409	384	−5.28	258	−0.27
star-24	444	+6.55	410	387	−6.42	258	−0.34

[a] Wavelength (in nm) of maximum dichroic absorption. [b] $\Delta\epsilon$ expressed in L mol^{-1} cm^{-1} and calculated for one repeating unit in the polymer. [c] Wavelength (in nm) of the crossover of dichroic bands. [d] Reference 8.

in Table 3, are quite close to those obtained for poly[(*S*)-MAP][8] prepared by AIBN free radical polymerization and for the analogous linear macromolecular derivatives obtained by ATRP,[18] reported for comparison. These results confirm that the process follows a Bernoullian statistics, as indicated by the similarity of $P_{m/r}$ with $P_{m/m}$ and of $P_{r/m}$ with $P_{r/r}$ (Table 3) as well as by the sum equal to one of $P_{m/r}$ with $P_{r/r}$ and of $P_{m/m}$ with $P_{r/m}$.[48]

Thus, the main-chain microstructure is essentially atactic, with a predominance of syndiotactic triads ($rr = 51-56\%$) suggesting a substantially low stereoregularity of the main chain. The ATRP of (*S*)-MAP starting from a rigid aromatic initiator is therefore poorly stereoselective, to a similar extent as the AIBN-initiated polymerization, and hence is unable to favor a strongly predominant tacticity of the macromolecules.

To investigate in more detail the conformational dissymmetry of these materials, the star polymers have been submitted to CD spectroscopy in $CHCl_3$ solution, in the spectral region between 250 and 700 nm (Table 4 and Figure 5b).

All the samples display two intense dichroic bands of opposite sign and slightly different intensity in correspondence of the first UV−vis absorption band, with a crossover point close to the wavelength of maximum absorption (407−410 nm). Such a behavior is typical of exciton splitting originated by cooperative interactions between side-chain azoaromatic chromophores disposed according to a mutual chiral geometry of one prevailing handedness.[8,49] By contrast, the CD spectrum of model (*S*)-PAP displays only two weak bands at 410 and 258 nm, related to the UV−vis absorptions, indicative of the absence of the above interactions as a consequence of the lack of any structural restriction.

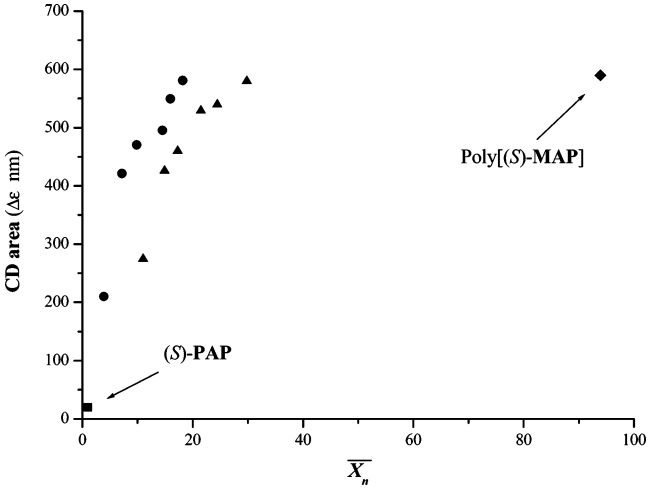

Figure 7. Evolution of the amplitude of the CD exciton couplet vs $\bar{X}_{n,SEC}$ of the star polymers (●) and the analogous linear derivatives previously synthesized[18,19] by ATRP (▲). The related values of (*S*)-PAP (■) and linear poly[(*S*)-MAP] with $\bar{M}_n = 31\,500$ (◆) are also represented.[8]

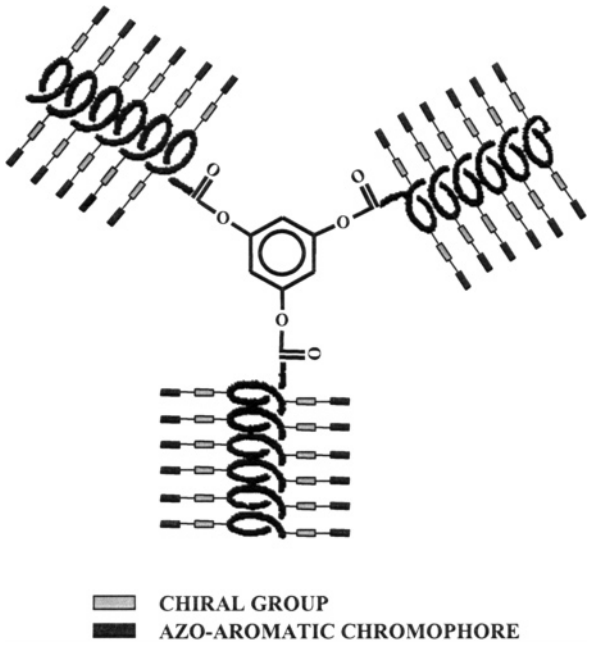

Figure 8. Idealized structure of optically active star polymers.

It is to be noted that the CD spectra display increasing amplitudes with the average molecular weight (Figure 5b). Therefore, as suggested also by the optical activity values, these polymeric derivatives, unlike the corresponding model compound, can assume, in dilute solution, at least for chain sections, a conformational dissymmetry of one prevailing screw sense whose extent depends on the average polymerization degree $\bar{X}_n$.

To evaluate the amount of dissymmetric conformations assumed by the macromolecules in solution, the integrated areas of the dichroic bands connected to the first UV−vis absorption band are reported in Figure 7 as a function of the average polymerization degree of the branched compounds and compared with the related data of the linear analogues obtained by AIBN free radical polymerization[8] and by ATRP.[18]

The dichroic amplitude values appear strongly dependent on the average molecular weight, their extent reaching a maximum value after which they remain approximately constant, in agreement with the results obtained by polarimetry. Furthermore, it is to be noted that at equal average polymerization degree

the star-shaped polymers show higher optical activity than the corresponding linear derivatives, the difference decreasing with the enhancement of $\bar{X}_n$.

This finding can be attributed to the stiffness of aromatic core, which limits the free movements of one chain end, thus favoring the macromolecules to assume a more elevated conformational rigidity with respect to the related linear samples. As ideally represented in Figure 8, the presence of the side-chain pyrrolidine moiety of one absolute configuration in each repeating unit allows, in fact, the assumption by the three macromolecular arms of the same preferred chiral conformation with one prevailing helix sense. As the chains are covalently linked by one end to the central core, their mobility is reduced, and consequently the overall chirality of the material improved with respect to the related linear derivatives having polymerization degree comparable to that of one single branch of the star-shaped macromolecules. It cannot be excluded, also, that the single branches of the three-arm macromolecules assume an intramolecular orientation favoring the overall dissymmetry of the system.

Conclusions

A series of three-arm star-shaped poly[(*S*)-MAP]s with different average molecular weights and low polydispersity have been prepared by ATRP by solely changing the reaction duration. The living character of the ATRP process is confirmed by the linear molecular weight−monomer conversion dependence and the narrow molecular weight distribution. These polymeric derivatives, unlike the corresponding monomeric model compound, can assume, in dilute solution, at least for chain sections, a conformational dissymmetry of one prevailing screw sense whose entity depends on the average polymerization degree. At equal values of chain length, their optical activity is higher than that of the analogous linear derivatives, probably due to the presence of the central core which forces the macromolecular chains to assume enhanced conformational dissymmetry with consequent amplification of optical rotation values and chiroptical properties. Further research aimed at clarifying the structural features and the chiral amplitude of the above-described polymeric systems, particularly in the solid state, is currently in progress.

Acknowledgment. The financial support by MIUR (PRIN2004) and Consortium INSTM (FIRB2001 "RBNE-01P4JF") is gratefully acknowledged.

References and Notes

(1) Kajitani, T.; Okoshi, K.; Sakurai, S.; Kumaki, J.; Yashima, E. *J. Am. Chem. Soc.* **2006**, *128*, 708−709.
(2) Yashima, E.; Maeda, K.; Nishimura, T. *Chem. Eur. J.* **2004**, *10*, 42−51.
(3) Wilson, A. J.; Masuda, M.; Sijbesma, R. P.; Meijer, E. W. *Angew. Chem., Int. Ed.* **2005**, *44*, 2275−2279.
(4) Angiolini, L.; Caretti, D.; Giorgini, L.; Salatelli, E.; Altomare, A.; Carlini, C.; Solaro, R. *Polymer* **1998**, *39*, 6621.
(5) Angiolini, L.; Caretti, D.; Carlini, C.; Salatelli, E. *Macromol. Chem. Phys.* **1995**, *196*, 2737.
(6) Angiolini, L.; Caretti, D.; Giorgini, L.; Salatelli, E. *Macromol. Chem. Phys.* **2000**, *201*, 533.
(7) Angiolini, L.; Caretti, D.; Giorgini, L.; Salatelli, E. *Polymer* **2001**, *42*, 4005.
(8) Angiolini, L.; Caretti, D.; Giorgini, L.; Salatelli, E. *J. Polym. Sci., Part A: Polym. Chem.* **1999**, *37*, 3257.
(9) Angiolini, L.; Giorgini, L.; Salatelli, E. *e-Polym.* **2003**, *no. 037*.
(10) Carlini, C.; Angiolini, L.; Caretti, D. Photochromic optically active polymers. In *Polymeric Materials Encyclopedia*; Salamone, J. C., Editor-in-Chief; CRC Press: Boca Raton, FL, 1996; Vol. 7, pp 5116−5123.
(11) *Proceedings of the Symposium on Azobenzene-Containing Materials*, Boston MA, 1998, Natansohn, A., Ed.; *Macromol. Symp.* **1999**, *137*, 1−165.
(12) Verbiest, T.; Kauranen, M.; Persoon, A. *J. Mater. Chem.* **1999**, *9*, 2005.
(13) Hopkins, T. E.; Wagener, K. B. *Adv. Mater.* **2002**, *14*, 1703.
(14) Xie, S.; Natansohn, A.; Rochon, P. *Chem. Mater.* **1995**, *5*, 405.
(15) Angiolini, L.; Bozio, R.; Daurù, A.; Giorgini, L.; Pedron, D.; Salatelli, E. *Macromolecules* **2006**, *39*, 489.
(16) Angiolini, L.; Bozio, R.; Giorgini, L.; Pedron, D.; Turco, G.; Daurù, A. *Chem. Eur. J.* **2002**, *8*, 4241.
(17) Angiolini, L.; Benelli, T.; Bozio, R.; Daurù, A.; Giorgini, L.; Pedron, D. *Synth. Met.* **2003**, *139*, 743.
(18) Angiolini, L.; Benelli, T.; Giorgini, L.; Salatelli, E. *Polymer* **2005**, *46*, 2424.
(19) Angiolini, L.; Benelli, T.; Giorgini, L.; Salatelli, E. *Polymer* **2006**, *47*, 1875.
(20) Angiolini, L.; Benelli, T.; Giorgini, L.; Painelli, A.; Terenziani, F. *Chem.—Eur. J.* **2005**, *11*, 6053.
(21) Hawker, C. J.; Frechet, J. M. J. In *New Methods of Polymer Synthesis*; Ebdon, J. R., Eastmond, G. G., Eds.; Chapman & Hall: New York, 1995; Vol. 2, p 290.
(22) Simms, J. A.; Spinelli, H. J. In *Star Polymer Synthesis*; Hatada, K., Kitayama, T., Vogl, O., Eds.; Marcel Dekker: New York, 1997; Vol. 40, p 379.
(23) Wulff, G.; Zweering, U. *Chem. Eur. J.* **1999**, *5*, 1898.
(24) Chow, H. F.; Fok, L. F.; Mak, C. C. *Tetrahedron Lett.* **1994**, *35*, 3547.
(25) Seebach, D. G.; Herrmann, F.; Lengweiler, U. D.; Bachmann, B. M.; Amrein, W. *Angew. Chem., Int. Ed. Engl.* **1996**, *35*, 2795.
(26) Chang, H. T.; Chen, C. T.; Kondo, T.; Siuzdak, G.; Sharpless, K. B. *Angew. Chem., Int. Ed. Engl.* **1996**, *35*, 182.
(27) Lehn, J. M. *Angew. Chem., Int. Ed. Engl.* **1990**, *29*, 1304.
(28) Lorenzo, M. O.; Baddeley, C. J.; Muryn, C.; Raval, R. *Nature (London)* **2000**, *404*, 376.
(29) Moberg, C. *Angew. Chem., Int. Ed. (Engl.)* **1998**, *37*, 248.
(30) Matyjaszewski, K.; Xia, J. *Chem. Rev.* **2000**, *101*, 2921.
(31) Han, Y. K.; Dufour, B.; Wu, W.; Kowalewski, T.; Matyjaszewski, K. *Macromolecules* **2005**, *37*, 9355.
(32) Wang, X. Z.; Zhang, H. L.; Shi, D. C.; Chen, J. F.; Wang, X. Y.; Zhou, Q. F. *Europ. Pol. J.* **2005**, *41*, 933.
(33) Wang, X. Z.; Zhang, H. L.; Zhong, G.; Wang, X. Y. *Polymer* **2004**, *45*, 3637.
(34) Perrin, D. D.; Amarego, W. L. F.; Perrin, D. R. *Purification of Laboratory Chemicals*; Pergamon Press: Oxford, 1966.
(35) Haddleton, D. M.; Waterson, C. *Macromolecules* **1999**, *32*, 8732.
(36) Carlmark, A.; Vestberg, R.; Jonsson, E. M. *Polymer* **2002**, *43*, 4237.
(37) Matyjaszewski, K.; Miller, P. J.; Pyun, J.; Kickelbick, G.; Diamanti, S. *Macromolecules* **1999**, *32*, 6526.
(38) Angot, S.; Murthy, K. S.; Taton, D.; Gnanou, Y. *Macromolecules* **1998**, *31*, 7218.
(39) Zhao, Y. L.; Shuai, X. T.; Chen, C. F.; Xi, F. *Chem. Mater.* **2003**, *15*, 2836.
(40) Altomare, A.; Ciardelli, F.; Ghiloni, M. S.; Solaro, R.; Tirelli, N. *Macromol. Chem. Phys.* **1997**, *198*, 1739.
(41) Chiellini, E.; Solaro, R.; Galli, G.; Ledwith, A. *Macromolecules* **1980**, *13*, 1118.
(42) Majumdar, R. N.; Carlini, C. *Makromol. Chem.* **1980**, *181*, 201.
(43) Carlini, C.; Garzoni, F. *Polymer.* **1983**, *24*, 101.
(44) Tinoco, I., Jr. *J. Am. Chem. Soc.* **1960**, *82*, 4785.
(45) Okamoto, K.; Itaya, A.; Kusabayashi, S. *Chem. Lett.* **1974**, 1167.
(46) Ciardelli, F.; Aglietto, M.; Carlini, C.; Chiellini, E.; Solaro, R. *Pure Appl. Chem.* **1982**, *54*, 521.
(47) Peat, I. R.; Reynolds, W. F. *Tetrahedron Lett.* **1972**, 1359.
(48) McCord, E.; Anton, W. L.; Wilczek, L.; Ittel, S. D.; Nelson, L. T. J.; Raffell, K. D. *Macromol. Symp.* **1994**, *86*, 47.
(49) Ciardelli, F.; Carlini, C.; Solaro, R.; Altomare, A.; Pieroni, O.; Houben, J. L.; Fissi, A. *Pure Appl. Chem.* **1984**, *56*, 329.

MA060148O